Heat Transfer and Frictional Characteristics in Rectangular Channel with Inclined Perforated Baffles

Se Kyung Oh, Ary Bachtiar Krishna Putra, and Soo Whan Ahn

Abstract—A numerical study on the turbulent flow and heat transfer characteristics in the rectangular channel with different types of baffles is carried out. The inclined baffles have the width of 19.8 cm, the square diamond type hole having one side length of 2.55 cm, and the inclination angle of 5°. Reynolds number is varied between 23,000 and 57,000. The SST turbulence model is applied in the calculation. The validity of the numerical results is examined by the experimental data. The numerical results of the flow field depict that the flow patterns around the different baffle type are entirely different and these significantly affect the local heat transfer characteristics. The heat transfer and friction factor characteristics are significantly affected by the perforation density of the baffle plate. It is found that the heat transfer enhancement of baffle type II (3 hole baffle) has the best values.

Keywords—Turbulent flow, rectangular channel, inclined baffle, heat transfer, friction factor.

I. INTRODUCTION

LIKE ribs, jet impingement and other passive heat transfer enhancement methods, insertion of baffle in a cooling system has been used for various types of industrial applications such as internal cooling systems of gas turbine blades, electronic cooling devices, shell-and-tube type heat exchangers, thermal regenerators, and labyrinth seals for turbo-machines.

Among important studies, Tsay et al.[1] numerically investigated the heat transfer enhancement on a vertical baffle in backward facing step flow channel. the effect of the baffle height, thickness and the distance between the baffle and the backward facing step on the flow was studied. They found that an insertion of a baffle into the flow could increase the average Nusselt number by 190%. They also observed that the flow conditions and heat transfer characteristics are strong function of the baffle position. Berner et al.[2]-[3] obtained experimental result of mean velocity and turbulent distributions in flow around segmented baffles. Experimental investigation of the turbulent flow and heat transfer characteristics inside the periodic cell formed between segmented baffles staggered in a rectangular duct was studied by Habib et al.[4] Numerical prediction of the flow and heat transfer in channel with staggered fins were investigated by. Webb and Ramadhyani[5], Kelkar and Patankar[6], and Habib et al.[7]

TABLE I
NOMENCLATURE

Symbol	Quantity	Unit [a]
G_ω	production of ω	
P_k	production of k	
Y_ω	dissipation of ω	
k	turbulent kinetic energy	m^2/s^2
ρ	density	kg/m^3
ω	specific dissipation rate	$N/m^2 s$
μ	viscosity, kg/m s	kg/m s
μ_t	viscosity, kg/m s	kg/m s
σ_k, σ_ω	turbulent Prandtl number	

All of the previous investigations used the solid segmented baffles. Experimental study of Dutta and Dutta[8] on perforated baffles showed better heat transfer augmentation with perforations compared to that with a solid baffles, if the plate is attached to the heated surface and properly aligned in the direction of the flow.

Very few number of research work were conducted numerically to capture more detail of the fluid flow pattern and heat transfer phenomena in the channel with perforated baffle. Yang and Hwang [9] reported the numerical prediction of the turbulent fluid flow and heat transfer characteristics for rectangular channel with porous baffle. In this research the turbulent governing equation are solved by a control volume-based finite difference method with turbulent model associated with wall function to describe the turbulent structure. The numerical results indicate that the flow patterns around the porous- and solid -type were entirely different due to different transport phenomena, and it is significantly influences the local heat transfer distributions. The lack of research in numerical analysis that related with perforated baffle motivates the present study to analyze numerically the turbulent flow structure and associated heat transfer enhancement in the rectangular channel with solid- and perforated-type baffles. An experimental work is also performed to validate these numerical results. This work employs an inclined baffle with different perforation density, having the baffle width of 19.8 cm and the square diamond type holes having one side length of 2.55 cm. These baffles have the holes of up to 9 and the inclination angle of 5°. Turbulent convective heat transfer is analyzed using the Reynolds

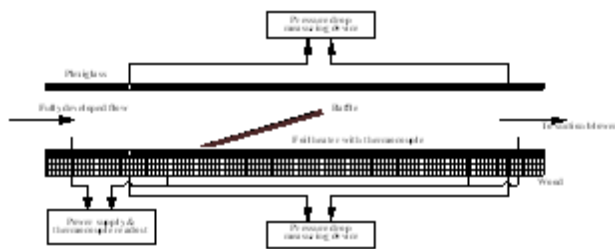Average Navier-Stokes (RANS) with SST turbulence model.

Fig. 1 Schematics of test apparatus

II. EXPERIMENTAL SET-UP

Fig. 1 shows a schematic diagram of the test apparatus. A suction-mode blower is used to draw air at room temperature through flow straighteners, passing through a long unheated straight rectangular channel with a cross-section of 19.8 cm (W)x 4 cm(H) and a length of 171.78 cm, finally through the heated test section of 71.2 cm. The channel has an aspect ratio of 4.95, and hydraulic diameter (D_h) of 6.66 cm. The entrance section is long enough to ensure a hydrodynamically fully developed flow just before the heated test channel. The left, right and upper sides of the channel are made of 5-mm-thick plexiglass plates, and the bottom side is made of 5-cm-thick wood plate.

A total of twenty three so-flux stainless steel foil heaters of the same size of 198 mm x 30 mm x 0.1 mm are mounted on the bottom surface of the test section. These foil heaters are aligned perpendicular to the flow direction and connected to a voltage controller to provide uniform heat flux. Twenty three copper constantan thermocouples are laid along the heated test section centerline and glued at each strip of the foil heater to measure the wall temperatures. Moreover, one thermocouple is placed at the inlet (10 cm upstream of the heated test section) and ten others are positioned at the outlet (9.2 cm downstream of the heated test section) to measure the inlet and outlet bulk air temperatures, respectively. Six pressure probes are used to measure pressure drops, and they are located at three positions of top, side, and bottom walls in 10 cm upstream of test section and three positions in 8 cm downstream of test section. Since the pressure taps are located upstream and downstream of the actual test section, a correction on the pressure drop is performed based on the smooth channel analysis by the micro-manometer (FCO-12, Furness Control Ltd). A row of impingement holes is placed along the centerline of the perforated baffle to match the thermocouple locations.

All baffle types are mounted on the heated wall have a constant inclination angle of five degrees and a gap of 4 mm between heated surface and the baffle is maintained to avoid flow stagnation. The baffle is placed at the position of 9.5 cm downstream from the start of the heated test section. Leading edge of the baffle is kept sharp to reduce possible flow disturbance by the protruding edge. In this study, all baffle types have the same overall size of length of 23.2 cm, width of 19.8 cm, and thickness of 5 mm, but different number of holes.

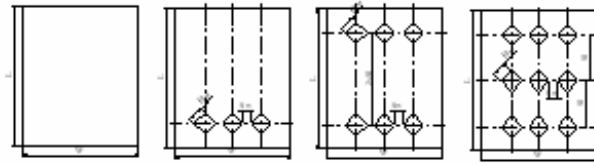Four different types such as the solid baffle (baffle type I),

Fig. 2 Baffle plate configuration

the 3 hole baffle (baffle type II), the 6 hole baffle (baffle type III), and the 9 hole baffle (baffle type IV) were dealt with, respectively. These square diamond type holes of width, H_w = 2.55 cm, transverse gap, S_w = 1.2 cm, and longitudinal gap, and S_l = 7.6 cm were manufactured as shown in Fig. 2. All of the thermocouples used in the experiment are carefully calibrated to an accuracy of 0.5 ^{o}C. The experimental uncertainties are estimated using the procedure outlined by Kline and McClintock[10]. The variables measured in this experiment are wall temperature, air temperature, velocity and pressure drop. It is found that the uncertainties for Reynolds number, friction factor and Nusselt number are about 2.5%, 9.5%, and 7.8%, respectively.
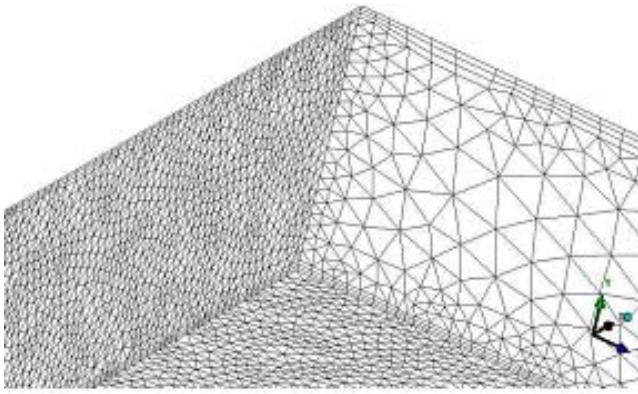
III. NUMERICAL MODELLING

A. Domain Model, Grid System, and Boundary Conditions

The numerical simulations are performed in three dimensional domain, which represents a rectangular channel with the inclined perforated-type baffle, as shown in Fig. 3. The software (ICEM CFD 10) is used to draw all parts in computational domain and to generate grid. The dimensions of computational domain are idealized to reveal the fundamental issues and enable validation with available experimental data that is the reason why this computational domain only cover the heated test section. This computational domain has a length, width, and height are the same size with the experimental model (L = 71.2 cm, W = 19.8 cm, and H = 4 cm). All of those baffle types such as, inclined solid-, inclined 3 hole-, inclined 6 hole-, and inclined 9 hole-type baffles are numerically simulated, and have the same size with the experimental model. Unstructured tetrahedral grid with prism smoothing near bottom wall, near top wall and near baffle surface are used to resolve high velocity gradient. The total number of nodes in those domains is more than 500,000 and total number of tetrahedrons is more than 1,500,000.
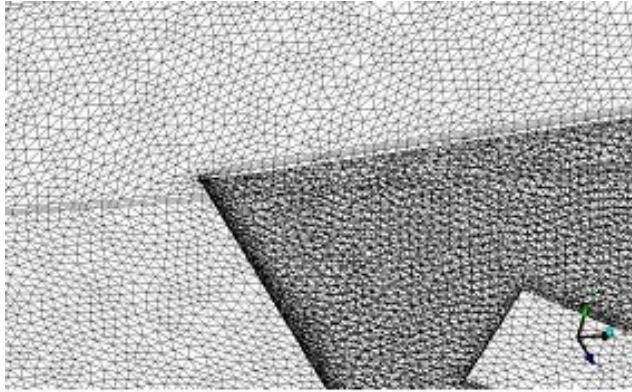
In the present numerical model, a uniform heat flux is specified on the bottom wall (heated wall), which defined at the same value with the experimental conditions. All walls in the rectangular channel except bottom wall are defined as an adiabatic wall.

B. SST Turbulent Model

The zonal modelling uses Wilcox's model near solid walls and Launder and Sharma's model near boundary layer edges and in free shear layers. This switching is achieved with a blending function F_1 of the model coefficients as follows:

(a) Channel wall

(b) Baffle plate

Fig. 3 Grid system mapping arrangements

Fig. 4 Grid independency test

$$h = \dot{Q}/\left[A(R_w - T_b)\right] \qquad (4)$$

where A is the total heat transfer area of the heated wall. The heat transfer rate () is defined as:

$$\dot{Q} = \dot{m}\, c_p\left(T_{b2} - T_{b1}\right) \qquad (5)$$

where T_{b1} and T_{b2} represent the fluid bulk temperatures at the entrance and exit, respectively. The local Nusselt number is defined using the local heat transfer coefficient and the hydraulic diameter D_h for the rectangular channel:

$$Nu = hD_h / k \qquad (6)$$

The local Nusselt number is normalized by the Nusselt number for fully developed turbulent flow in a smooth circular tube correlated by McAdams/Dittus-Boelter[13] as:

$$Nu / Nu_{ss} = (hD_h / K)/\left(0.023\, \mathrm{Re}^{0.8}\, \mathrm{Pr}^{0.4}\right) \qquad (7)$$

The Reynolds number was calculated on the basis of channel average velocity and channel hydraulic diameter. The channel average velocity was obtained from the flow rate of the circular tube at downstream of test section

V. RESULTS AND DISCUSSION

For verifying the grid independence of the predicted results, a grid resolution study has been carried out for the rectangular channel with single solid baffle (baffle type I), at the Reynolds number of 23,000, as shown in Fig. 4. The differences were found to be minor in the range of the node number of 329,688 to 568,755. The node number of 568,755 has been used in the solid baffle (baffle type I). The present experimental

SST model = $F_1.$ ($k - \omega$ model)
        + (1-F_1).($k - \varepsilon$ model) $\qquad (1)$

where the standard $k - \omega$ was first proposed by Wilcox[11] as follows:

$$\frac{\partial}{\partial t}(\rho k) + \frac{\partial}{\partial x_i}(\rho k u_i) = \frac{\partial}{\partial x_j}\left[\left(\mu + \frac{\mu_t}{\sigma_k}\right)\frac{\partial k}{\partial x_j}\right] + P_k - \beta^* \rho k \omega \qquad (2)$$

$$\frac{\partial}{\partial t}(\rho \omega) + \frac{\partial}{\partial x_i}(\rho \omega u_i) = \frac{\partial}{\partial x_j}\left[\left(\mu + \frac{\mu_t}{\sigma_\omega}\right)\frac{\partial \omega}{\partial x_j}\right]$$
$$+ G_\omega - Y_\omega + (1 - F_1)D_\omega \qquad (3)$$

And $k - \varepsilon$ model was used by Launder and Sharma's model[12].

IV. DATA REDUCTION

The local heat transfer coefficient is calculated from the net heat transfer rate per unit surface area exposed to the cooling air, the local wall temperature (T_w), and the local bulk mean air temperature (T_b) as follows:
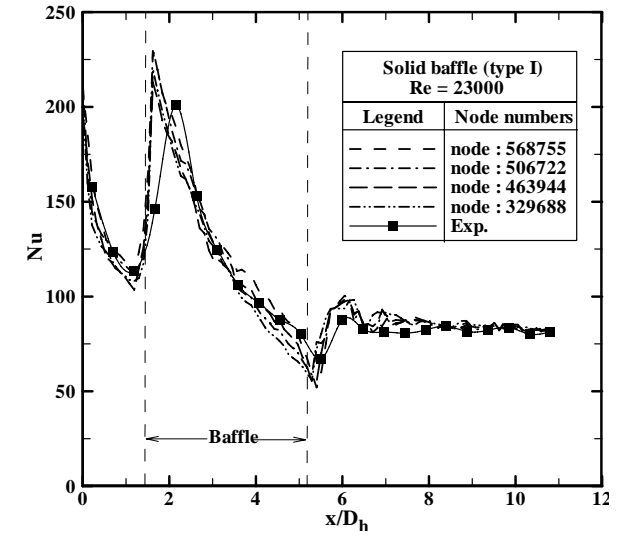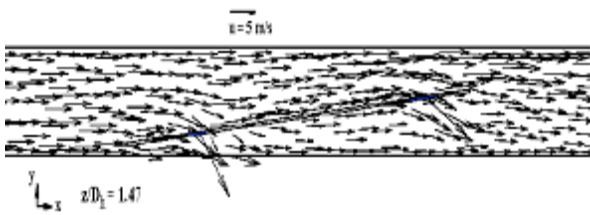
Fig. 5 Flow field (x-y surface, z/D_h =1.47) on the baffle type III

(a)

(b)

Fig. 7 Isotherms on the cutting plane at y-z surface
the baffle type III at Re = 23,000

data do not precisely match the numerical results. It is not surprising because the discrepancies between calculated and measured results may be attributed to the variable fluid properties and the possible influence of buoyancy in the experimental system. In addition, as mentioned earlier, one thermocouple in each heater gives the local wall temperature at channel centerline (location of jet impingement) and therefore, presented results do not reflect span-averaged Nusselt number characteristics.

The local Nusselt number is comparatively higher at the start of heating section due to the steeper development of the thermal boundary layer. The local Nu peaks take place at the dimensionless axial location of x/D_h = 2.2 because the gap between the baffle leading edge and the heating wall (bottom wall) generates the flow acceleration and flow impingement.

Fig. 5 shows the flow field of two impinging jets on x-y surface in the baffle type III; i. e., first impingement is produced by the three holes at the first row of holes at the dimensionless axial location of x/D_h = 2.18. And second impingement is also produced by the second row of holes at x/D_h = 4.46 downstream from the start of the heater. Fig. 6 shows fluid
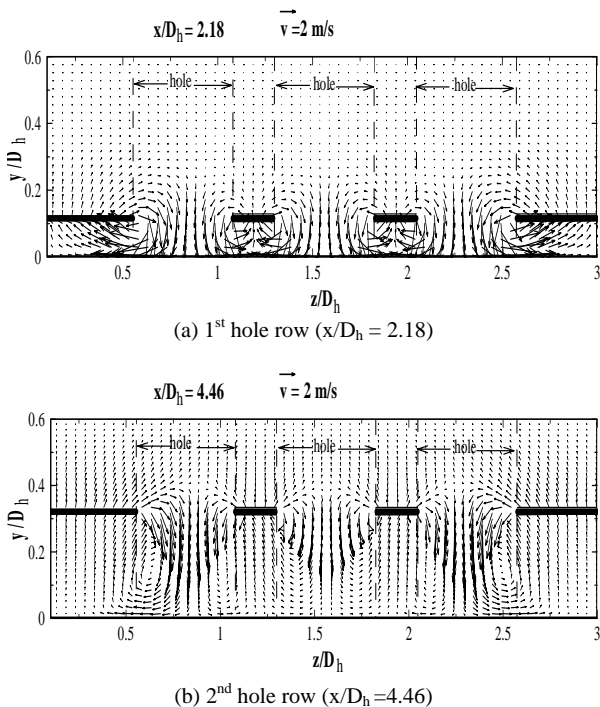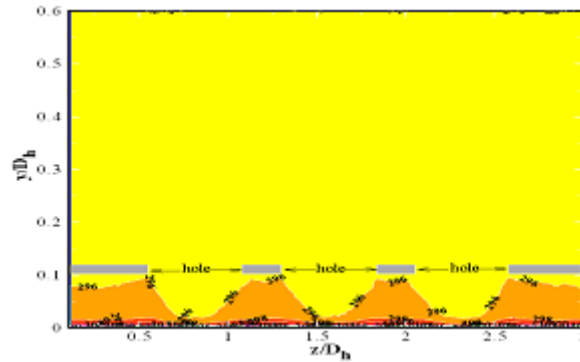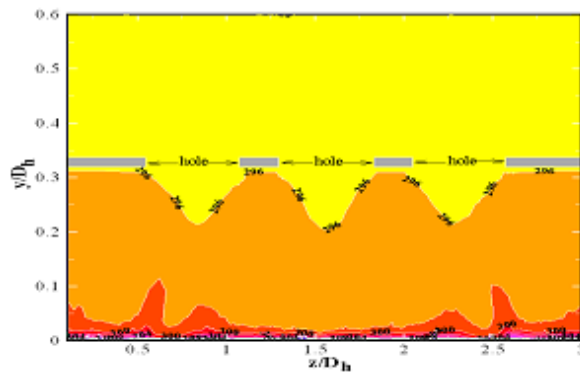

(a) 1st hole row (x/D_h = 2.18)

(b) 2nd hole row (x/D_h =4.46)

Fig. 6 Fluid flow pattern on the cutting plane of the baffle type III
at Re = 23000

flow patterns on the cutting-plane at 1st hole row (x/D_h = 2.18) and) 2nd hole row (x/D_h = 4.46) in baffle type III. At the 1st row of x/D_h =2.18 the velocity vectors around the holes are greater than those in the 2nd row of x/D_h=4.46. It means that the impinging jet flow become stronger at closer distance near the holes, and became weaker at the farther distance.

Fig. 7 shows the isotherms at the cutting plane of the first row and second row of holes (x/D_h = 2.18 and x/D_h = 4.46). As the same is true with fluid flow patterns in Fig. 6, the temperature gradient on the impact surface at the second row location is also less than those at the first location. It must be noted that the characteristics of temperature distributions relate the fluid flow pattern.

Fig. 8 shows that the local Nusselt number distributions of the channel for baffle type III at Reynolds number of 23,000. Comparing to the baffle type I of Fig. 4, the first peaks of Nusselt number in the baffle type III of Fig. 8 are

lower. It is due to the fact that cross flow by spent jets is stronger for the perforated plate and reduces impingement effect. Moreover, due to higher flow resistance in the baffle type I, more air passes through the gap between the baffle and the bottom surface. Therefore, this increases the reattachment heat transfer coefficient. And the peaks occur earlier in the solid baffle than those of perforated baffle. It can be argued that flow passing through impingement chamber is stronger in perforated baffle and as a result the bypass flow not participating in impingement is weaker and thus reattachment is delayed.
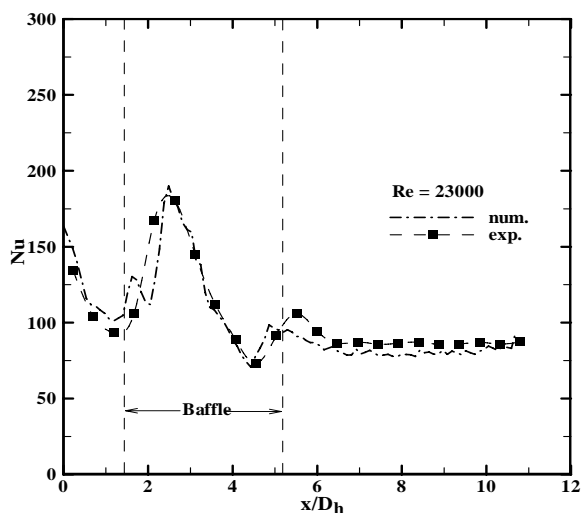
Fig. 8 Centerline local Nusselt number for the baffle type III at Re = 23,000

Seyedein et al.[14] numerically investigated the jet-deflection by cross-flow in a converging confinement chamber. However, the present configurations have a divergent confinement chamber. Because the flow area increases in a divergent chamber, the cross flow is weaker than a non-divergent channel. Therefore, the distance of the target surface increases from the issuing jet. The advantage of this divergent configuration is its ability to be accommodated in a a periodic fashion.

Fig. 9 shows the channel-averaged friction factors obtained from the experimental and numerical data for all baffle types. The friction factor of the solid baffle (baffle type I) is greatest due to more blockage of bulk flow caused by inserting this baffle, leading to greater friction value. The empirical equation by Blasius for a smooth circular tube [13] is included for a comparison. Our results for a smooth channel with no baffle coincide well with the Blasius' correlation. The friction factor
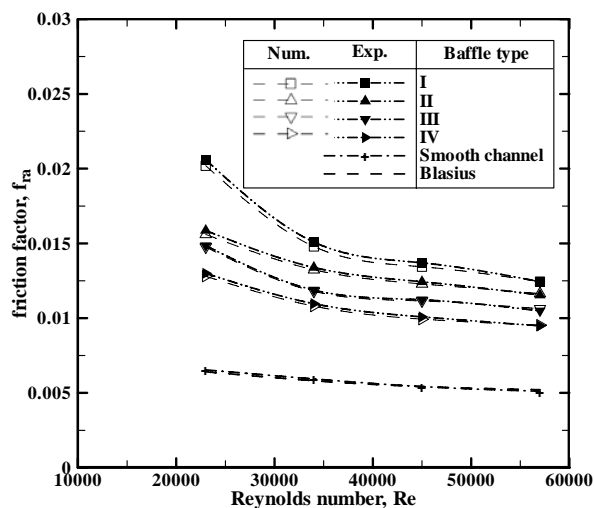
decreases with increasing Reynolds number since a relative increase in the magnitude of the kinetic energy is greater than a increase in the wall shear stress.

VI. CONCLUSION

The characteristics of fluid flow and heat transfer in a rectangular channel with single inclined baffle and the flow Reynolds number is varied between 23,000 and 57,000 are numerically and experimentally investigate. Listed below are major findings:

1) Numerical predictions of the flow fields and isotherms depict that each baffle has a different transport phenomenon.
2) The solid-type (type I) baffle channel has the highest friction factor due to more flow blockage.
3) The Nusselt number are greatest at the baffle type II.

REFERENCES

[1] Y. L. Tsay, T. S. Chang, J. C. Cheng, "Heat transfer enhancement of backward-facing step flow in a channel by using baffle installed on the channel wall", Acta Mech., 2005, Vol 174, pp. 63-76..
[2] C. Berner, F. Durst and D. M. McEligot, "Flow around baffles", ASME J. Heat Transfer, 1984, Vol. 106, pp. 743 -749.
[3] C. Berner, F. Durst and D. M. McEligot, "Streamwise-periodic flow around baffles", Proceeding of the 2nd Int. Conf. on Applications of Laser Anemometry to Fluid Mechanics, Lisbon, Portugal, 1984.
[4] M. A. Habib, A. M. Mobarak, M. A. Sallak, E. A. Abdel Hadi and R. L. Affify, "Experimental investigation of heat transfer and flow over baffles of different heights", ASME J. Heat Transfer, 1994, Vol. 116, No. 2, pp. 363-368.
[5] B. W. Webb, and S. Ramadhyani, "Conjugate heat transfer in a channel with staggered ribs", Int. J. Heat Mass Transfer, 1985, Vol. 28, pp. 1679-1687.
[6] K. M. Kelkar, and S. V. Patankar, "Numerical prediction of flow and heat transfer in parallel plate channel with staggered fins", Trans. ASME J. Heat Transfer, 1987, Vol. 109, pp. 25-30.
[7] M. A. Habib, A. E. Attya and D. M. McEligot, "Calculation of turbulent flow and heat transfer in channels with streamwise-periodic flow", Trans. ASME J. Turbomach., 1988, Vol. 110, pp. 405-411.
[8] P. Dutta and S. Dutta, "Effect of baffle size, perforation and orientation on internal heat transfer enhancement", Int. J. Heat Mass Transfer, 1998, Vol. 41, No. 19, pp. 3005-3013.
[9] Y. T. Yang and C. Z. Hwang, "Calculation of turbulent flow and heat transfer in a porous-baffled channel", Int. J. Heat Mass Transfer, 2003, Vol. 46, pp. 771-780.
[10] S. J. Kline and F. A. McClintock, "Describing uncertainty in single sample experiments", Mechanical Engineering, 1953, Vol. 75, pp. 3-8.
[11] D. C. Wilcox, Turbulent modelling for CFD. 2nd ed., DCW Industries. 1998.
[12] B. E. Launder and B. L. Sharma, "Application of the energy-dissipation model of turbulence to the calculation of flow near a spinning disc", Letters in Heat and Mass Transfer, 1974, Vol. 1, Issue 2, pp. 131-137.
[13] W. M. Kays and M. E. Crawford, "Convective heat and mass transfer", 2nd ed., McGraw-Hill, New York. 1990.
[14] S. H. Seyedein, M. Hasan, and A. S. Mujumdar, "Laminar flow and heat transfer from multiple impinging slot jets with an inclined confinement surface", Int. J. Heat and Mass Transfer, 1994, Vol. 37, pp. 1867-1875.

Se Kyung Oh was born on March 06, 1948, Yi-Sung, Kyungbuk, South Korea. Doctor in hydraulic engineering from Pukyong National University, Busan, South Korea. Ary Bachtiar Krishna Putra, Ph.D is student in Gyeongsang National University, Tongyong, South Korea. Soo Whan Ahn is Doctor in heat

Fig. 9 Friction factor

transfer from Busan National University, Busan, South Korea. Manuscript submitted October 27, 2008

Se Kyong was with Mechanical and System Engineering, Gyeongsang National University, 445 Inpyongdong - Tongyong, South Korea, as professor on hydraulic engineering area. Ary Bachtiar Krishna Putra was PhD. Student in Mechanical and System Engineering, Gyeongsang National University, 445 Inpyongdong - Tongyong, South Korea. Soo Whan Ahn was with Mechanical and System Engineering, Gyeongsang National University, 445 Inpyongdong – Tongyong, South Korea, as professor on heat transfer area.